

## MANIPULATION OF THE MICRO AND MACRO-STRUCTURE OF BEAMS EXTRACTED FROM CYCLOTRONS

R.E. Laxdal

*TRIUMF, 4004 Wesbrook Mall, Vancouver, B.C., Canada V6T 2A3*

It is standard practice in cyclotrons to alter the extracted micro-pulse width by using center-region slits and/or by chopping the beam before injection. The macro-structure can also be varied by means of pulsed or sinusoidal deflection devices before injection and/or after extraction. All above methods, however, involve cutting away the unwanted beam, thus reducing the time-averaged intensity. This paper will focus on some methods used to alter the time structure of extracted beams without significant beam loss. For example radial gradients in the accelerating fields from rf cavities can be utilized to compress, expand or even split longitudinally the circulating particle bunches. The macro-structure of the extracted beam can be altered by employing resonant extraction methods and replacing the static magnetic bump with either a pulsed or a sinusoidal transverse perturbation. The methods are most suitable for  $H^-$  cyclotrons but may also be considered in a limited scope for cyclotrons using direct extraction. Results of computer simulations and beam tests on the TRIUMF 500 MeV  $H^-$  cyclotron will be presented.

### 1 Introduction

Cyclotrons typically operate in cw mode, with rf frequencies in the 10-50 MHz range and with beam bunches occupying up to  $40^\circ$  of each rf cycle. For certain applications (i.e. injection into a post-accelerator, time-of-flight measurements, experiments investigating certain rare decays) it may be desirable to alter either the micro-structure (within the rf period) or the macro-structure (over several rf periods) of the extracted beam. For cyclotrons with external injection systems it is a standard practise to bunch longitudinally the beams prior to injection to improve the percentage of the beam accepted into the longitudinal phase space. Beyond this the customizing of the timing of the extracted beam pulses largely comes from cutting away the unwanted beam. Slits or flags on the first turns can be used to trim the longitudinal extent of the bunch to help reduce phase-dependent turn broadening and tailor the micro-pulse length of the extracted beam. The macro-structure of the extracted beam can be selected with a pulsed deflection scheme in the injection beamline. Pulsed deflectors in the extraction line can also be used to clean up the macro-pulses.<sup>1</sup>

In some cases, however, it is essential that the longitudinal structure of the extracted beam be altered but with no reduction in the average current. Barring then any increase in the injected current the unwanted beam cannot be cut but must only be re-distributed longitudinally. In this paper we explore a few methods that can be utilized to alter the time distribution of the extracted beam with little or no reduction in the extracted intensity. The 500 MeV TRIUMF cyclotron is used to illustrate the techniques but they are applicable to other cyclotrons as well. In some cases the re-distribution in phase space that accompanies the longitudinal re-distribution precludes efficient direct extraction since separated turns would be lost.

### 2 TRIUMF Cyclotron

The TRIUMF cyclotron accelerates  $H^-$  ions at an rf frequency of 23 MHz, a fifth harmonic of the orbit frequency, 4.6 MHz, with five particle bunches per turn. Typically, 160  $\mu A$  are accelerated to 500 MeV with extraction by stripping. These ions occupy  $30-40^\circ$  of the rf cycle. Hence the time structure of the extracted beam in cw mode consists of 4-5 nsec pulses separated by 43 nsec. A first and second harmonic buncher in the injection line are routinely used and give a transmission from injection to extraction of  $\sim 60\%$ . From space charge considerations, the maximum allowable average intensity in the TRIUMF cyclotron without major development is 10  $\mu A/^\circ$  of rf or  $\sim 400 \mu A$ .<sup>2</sup>

Presently the separation between output pulses can be increased five-fold with a corresponding reduction in the average current by cancelling four of the five particle bunches before injection. In addition the macro-duty cycle can be altered by a 1 kHz pulser in the injection line giving bursts of variable length separated by up to 1 msec. The energy spread in the turns, produced by the phase-dependence in the acceleration, as well as the low radius gain per turn (1.5 mm at 500 MeV) cause overlapping of turns and a uniform radial beam density. At full intensity the energy spread in the extracted beam is  $\sim 1$  MeV with transverse emittances of  $(\epsilon_x, \epsilon_z) = (1\pi, 2\pi) \mu m$ .

### 3 Splitting Micro-pulses with Higher Harmonic Cavities

To match a cyclotron to a higher frequency post-accelerator such as a cw superconducting linac<sup>3</sup>, it is necessary to increase the bunch frequency and decrease the bunch length. At linac operating frequencies of 200 MHz and above, a typical micro-pulse from a cyclotron would

be much too large. The phase expansion effect, using higher harmonic rf cavities, can, in principle, increase the frequency of the cyclotron bunches by a factor of 6-8 or more while simultaneously compressing the bunches longitudinally to a phase width compatible with linac acceleration.<sup>4</sup>

### 3.1 Phase Compression/Expansion

A radial gradient in the accelerating field from an rf cavity gives rise to a time-varying magnetic field 90° out of phase with the accelerating field. These magnetic fields are responsible for the phase compression/expansion effect.<sup>5,6</sup> Positive radial gradients focus or compress off-phase particles longitudinally, while negative gradients defocus or expand the bunch length. The amount of longitudinal phase change per turn is given by

$$\frac{d\phi}{dn} = \phi_{ni}(E) - \frac{dE_{G1}}{dE} \sin \phi - \sum_m \frac{1}{m} \frac{dE_{Gm}}{dE} \sin m(\phi - \phi_m)$$

where  $E_{G1}$  is the peak energy gain per turn from the fundamental,  $E_{Gm}$  is the peak energy gain per turn from a cavity operating at the  $m^{\text{th}}$  harmonic,  $\phi_m$  is the phase of the  $m^{\text{th}}$  cavity with respect to the fundamental and  $\phi_{ni}$  is the phase slip per turn due to non-isochronism.

Assuming an isochronous situation (i.e.  $\phi_{ni} = 0$ ) and the addition of an extra cavity of harmonic  $m$ , a particle's phase,  $\phi_f$ , can be determined at any energy from the initial values of the peak energy gain per turn  $E_{G1}(R_o)$ , and phase  $\phi_o$ , by solving

$$E_{G1}(R_o) \sin \phi_o = E_{G1}(R_f) \sin \phi_f + \frac{E_{Gm}(R_f)}{m} \sin m(\phi_f - \phi_m).$$

Where the extra cavity is phased to accelerate (i.e.  $m\phi_m = 0$ ), longitudinal bunching will occur. When phased to oppose the fundamental acceleration (i.e.  $m\phi_m = 180^\circ$ ), and when  $E_{Gm}(R_f)/E_{G1}(R_f)$  is less than unity, the added cavity expands the accelerated phase band.

### 3.2 Phase-splitting

For cases where the peak energy gain per turn from the opposing cavity exceeds that from the fundamental an unstable fixed point occurs in phase space at the energy at which  $E_{Gm}(E) = E_{G1}(E)$  and phase  $\phi = 0$ . Particles slightly off-phase are funneled past the fixed point skirting around a forbidden region defined by

$$\frac{m \cdot \sin \phi}{\sin m\phi} = \frac{E_{Gm}(E)}{E_{G1}(E)}.$$

The final phases for particles of  $\phi_o = 0^+$  and  $\phi_o = 10^\circ$  are plotted for various harmonics and for various energy gain ratios in Fig. 1. These values define the limits of the positively split bunch for a beam of initial phase width  $\pm 10^\circ$ . The  $\phi_o = 10^\circ$  results assume  $E_{G1}(R_o) = E_{G1}(R_f)$ . Note

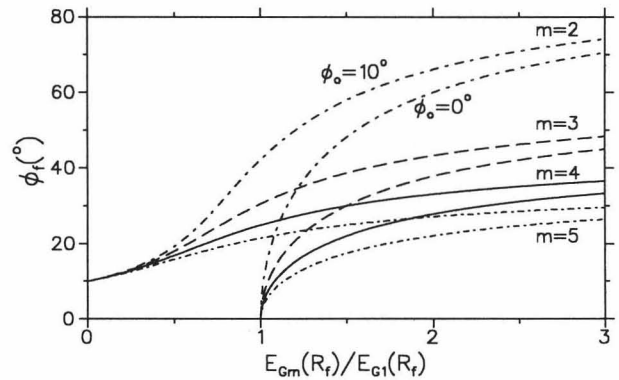


Figure 1: Final phase values for particles of initial phase  $\phi_o = 0^+, 10^\circ$  resulting from the addition of a higher harmonic cavity ( $m = 2, 3, 4$ , or  $5$ ) with peak energy gain  $E_{Gm}$  and phase opposing the fundamental. The  $\phi_o = 10^\circ$  results assume  $E_{G1}(R_o) = E_{G1}(R_f)$ .

that the separation of the positive bunch from the negative bunch increases, and the bunch width decreases for an increasing cavity voltage. Also as the cavity harmonic increases the bunch separation decreases.

Fig. 1 can be used to estimate the specifications of an additional  $\lambda/4$  cavity to better match the longitudinal cyclotron bunch structure to a higher frequency linac. As an example an additional  $2^{\text{nd}}$  harmonic cavity, with a peak energy gain 1.8 times that provided by the fundamental and of reverse phase would split the  $\pm 10^\circ$  phase band into two  $\sim 7^\circ$  bands separated by  $120^\circ$ . The compressed bunches would be compatible with injection into a linac of frequency six times that of the cyclotron ( $h_L = 6$ ), with two out of six buckets filled; the particles occupying  $\sim 40^\circ$  of the linac bucket. In a similar way single cavities of different specifications can be used to achieve phase band separations and bunch lengths compatible with other linac frequencies. For example separations of  $90^\circ$  or  $45^\circ$  are both compatible with  $h_L = 8$ .

To populate more of the linac buckets another cavity of higher harmonic can be added to produce two other unstable fixed points, symmetric about  $\phi = 0$ , to further split the two bunches. A simple impulse approximation code was written to simulate longitudinal dynamics in the TRIUMF cyclotron. The code was used to estimate the specifications and positions of cavities to match into a time structure 6 and 8 times higher than the cyclotron fundamental.<sup>4</sup> For simplicity, perfect isochronism was assumed as well as a uniform fundamental dee voltage of 80 kV, yielding  $E_{G1} = 320$  keV. In all cases the additional higher harmonic cavities were  $\lambda/4$  type; the energy gain rising in a cosine with radius. In Fig. 2 ten particles of initial phase  $\pm 10^\circ$  are accelerated and displayed once every one hundred turns. Additional  $2^{\text{nd}}$  and  $3^{\text{rd}}$  harmonic cavities yield three output bunches separated by

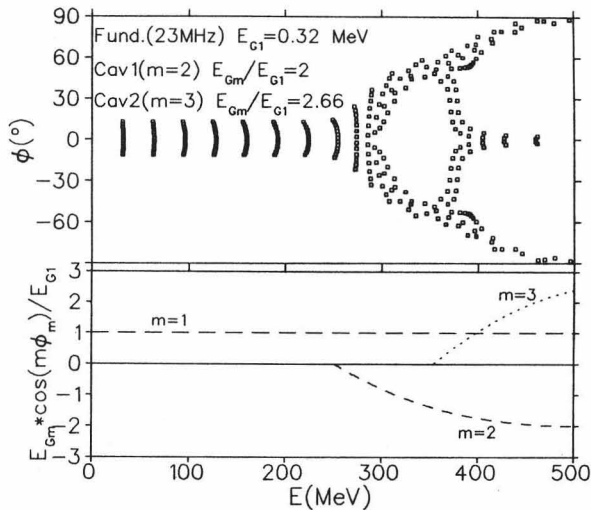


Figure 2: The bottom figure shows the effective energy gain per turn, normalized to the energy gain of the fundamental, for the fundamental, and additional 2<sup>nd</sup> and 3<sup>rd</sup> harmonic  $\lambda/4$  cavities as a function of energy. In the top figure particle trajectories in  $(E, \phi)$  space, plotted every one hundred turns, show how the initial phase band of  $\pm 10^\circ$  is split into three  $\sim 4^\circ$  bands separated by  $90^\circ$ .

$90^\circ$ , compatible with  $h_L = 4$  or  $h_L = 8$ . If a third, 8<sup>th</sup> harmonic cavity, contributes to the acceleration, four phase bands separated by  $45^\circ$  that would fill four linac buckets out of eight for each cyclotron pulse are produced. The resultant particle trajectories are plotted in  $(R, \theta)$  space in Fig. 3. The linac buckets are superimposed on the plot.

In an actual application the extracted population densities in phase space would depend on the details of isochronism and on the stability of the rf and magnetic fields. Clearly the technique would destroy any separated turn structure, reducing the extraction efficiency for proton cyclotrons. In addition the increased energy gain per turn would produce a larger energy spread in the extracted beam.

### 3.3 Test Results

A fourth harmonic  $\lambda/4$  auxiliary accelerating cavity<sup>7</sup> (AAC) was installed in the TRIUMF cyclotron in 1990 to augment the fundamental energy gain per turn, and hence reduce losses, in the energy range from 350 – 500 MeV. At full voltage (140 kV) it provides a maximum energy gain 0.88 times the existing maximum energy gain. When phased to provide additional acceleration, the length of the extracted bunch is reduced by phase compression from the 3.8 nsec to 2.1 nsec in agreement with the relation of Sec. 3.1.<sup>8</sup>

To produce the phase-splitting effect the isochronism was shifted from the ideal (by adjusting the rf frequency),

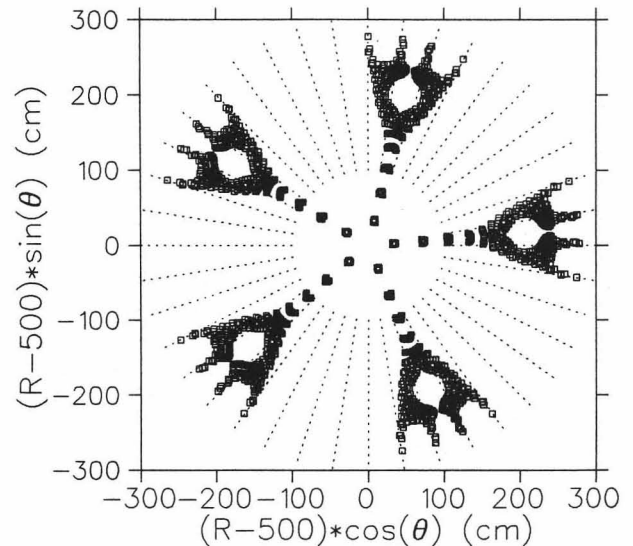


Figure 3: Shown are the five particle bunches per turn in TRIUMF, starting from 500 cm ( $E = 140$  MeV), and splitting into four bunches per spoke with the influence of the higher harmonic cavities; a 2<sup>nd</sup>, 3<sup>rd</sup>, and 8<sup>th</sup>. Superimposed on the plot are the linac buckets, eight times the cyclotron frequency.

reducing the effective energy gain from the fundamental while the AAC was phased to oppose the circulating beam.<sup>8</sup> A final time spectrum of the resulting extracted beam compared to the time structure with the cavity off is shown in Fig. 4. Complete phase-splitting is evident with the two sub-bunches separated by 7.6 nsec.

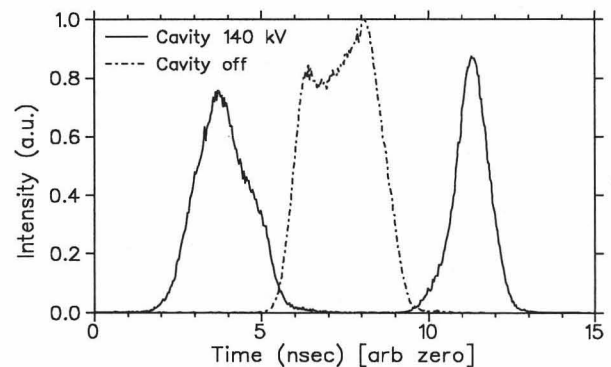


Figure 4: Experimental result showing the time spectrum of beam extracted from the TRIUMF cyclotron with (solid line) and without (dotted line) an additional 4<sup>th</sup> harmonic cavity ( $E_{G4}(R_f)/E_{G1}(R_f) = 0.88$ ) phased to oppose the circulating beam.

## 4 Stacking Micro-pulses by Resonant Extraction

### 4.1 Resonant Coherent Growth

A standard technique to enhance the efficiency of extracting with an electro-static septum system is to add a precessional component to the radius gain per turn. A static first harmonic magnet bump is used to generate a coherent radial oscillation at  $\nu_r=1$ . Subsequent precession of the beam in radial phase space produces a modulation in the radius gain per turn.

A pulsed field can also be used to excite the beam at a non-integer resonance. For cases where  $1/(\nu_r - 1) = N_s$ , an integer, a coherent growth can develop if the beam is driven by a radial pulsed field of frequency  $\omega_{pulse} = \omega_{ion}/N_s$  where  $\omega_{ion}$  is the particle orbit frequency. In this case the radial phase space vector advances  $2\pi$  every  $N_s$  turns and the perturbations will add cumulatively. We call  $N_s$  the *stacking factor* for reasons that will become obvious. The perturbing field would span the resonance region and in the simplest case the pulse on time would correspond to a complete orbital period. The pulse would simultaneously increment the coherent amplitude of all particles in the resonance region once every  $N_s$  turns. Therefore every particle in an  $N_s$  radial range will have a similar coherent amplitude. The situation is the same for vertical perturbations at positions where  $1/\nu_z = N_s$ . A pulsed field with a period of  $N_s=4$  turns is shown in Fig. 5(b) compared to a circulating beam of five bunches per turn (Fig. 5(a)).

Next consider a sinusoidal perturbing field. In the general case,  $h$  particle bunches per turn circulate in a cyclotron, where  $h = \omega_{rf}/\omega_{ion}$  and  $\omega_{rf}$  is the accelerating frequency. Since, in this case, the perturbing field is varying, bunches on the same turn see different deflection amplitudes (Fig. 5(c)). However each bunch receives identical deflections averaged over  $N_s$  turns if the perturbation frequency  $\omega_{perturb} = h\omega_{ion}/N_s$ , provided that  $h/N_s$  or  $N_s/h$  are not integers. The growth is somewhat more efficient than in the pulsed case since perturbations can drive the growth on every turn rather than once every  $N_s$  turns.

At the resonance, for either sinusoidal or pulsed perturbations, the time-integrated particle positions in the  $(x, p_x)$  or  $(z, p_z)$  phase space form  $N_s$  *spokes* spaced uniformly in phase angle,  $2\pi/N_s$  apart, increasing incrementally in length with every perturbation (Fig. 6). In the pulsed case one coherent position on a *spoke* corresponds to the bunches in an  $N_s$  turn spatial range that have been given identical cumulative perturbations and are synchronized in time. At any one time only one *spoke* is occupied. The sinusoidal case is similar except that different bunches may populate different *spokes* simulta-

neously. In both cases, at the azimuth of the deflector the peak perturbing field corresponds to the *spoke* on the positive momentum axes.

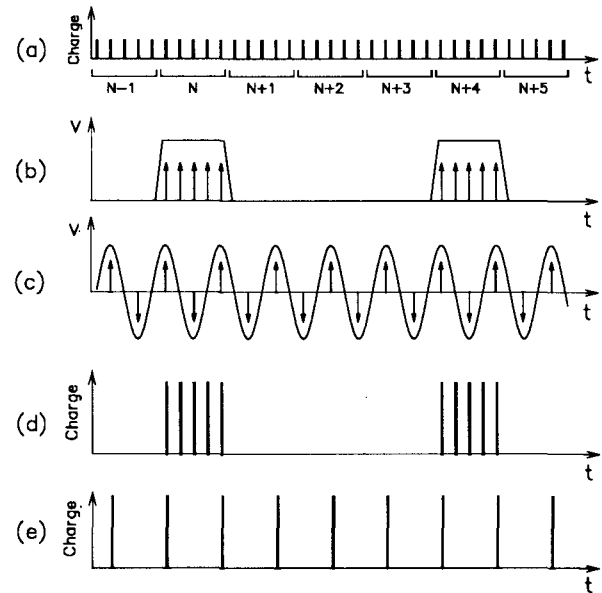


Figure 5: (a) Schematic showing the pulsed (b) and sinusoidal (c) fields required to create coherent growth at  $\nu_r=1.25$  or  $\nu_z=0.25$  for the  $h=5$  bunch per turn time structure shown in (a). The extracted time structures for both the pulsed field (d) and the sinusoidal field (e) are also shown.

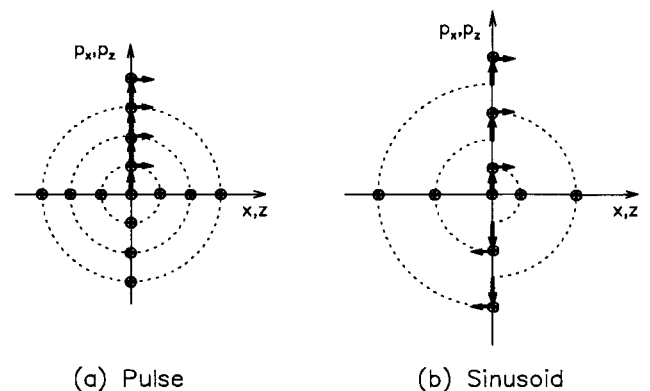


Figure 6: Schematic view of the motion in  $(x, p_x)$  or  $(z, p_z)$  at  $\nu_r=1.25$  or  $\nu_z=0.25$  for the deflecting fields shown in Fig. 5; in (a) from a pulsed field and (b) from a sinusoidal field. The vertical arrows show the particle deflections and the horizontal arrows indicate the direction of the  $2\pi/N_s$  phase advance.

Extraction at non-integer radial resonances by time-varying fields provides a way to improve extraction efficiency in cyclotrons where it is not practical or disadvantageous to drive the tune towards an integer. There is, however, another interesting application of the technique. Whether operating in a pulsed or sinusoidal mode

the  $N_s$  *spoke* positions are completely synchronized with the driving field. Hence if the extraction device, whether an electric septum or charge exchange foil, can be positioned to extract particles from a single coherent *spoke* then the extracted pulse frequency will be altered without loss of average beam intensity. For the pulsed field of Fig. 5(b) the extracted time structure would consist of  $h$  regularly separated bunches repeating every  $N_s$  turns (Fig. 5(d)). With a sinusoidal deflection every  $N_s^{\text{th}}$  bunch is extracted at a frequency of  $\omega_{rf}/N_s$  (Fig. 5(e)). In both cases each extracted bunch is sampled spatially from  $N_s$  neighbouring turns so is  $N_s$  times brighter than bunches extracted normally.

#### 4.2 Extraction of Resonantly Excited Beams

The coherent growth from a static deflection at  $\nu_r=1$  will precess  $\Delta\phi = 2\pi(\nu_r - 1)$  each turn. When superimposed on the radius gain due to acceleration, the precession produces a cycloidal pattern in radial phase space with the radial width of each cycle corresponding to  $1/(\nu_r - 1)$  turns. The radius gain is augmented by a precessional component with maximum amplitude of  $2A_c \cdot \sin\pi(\nu_r - 1)$  where  $A_c$  is the coherent amplitude. The extraction septum would be positioned in one of the cycles where the turn separation is maximized.

The coherent amplitude created in the pulsed or sinusoidal case will precess after the resonance with a phase advance of  $N_s \cdot 2\pi(\nu - \nu^*)$  every  $N_s$  turns where  $\nu^*$  is the non-integer transverse resonance where the growth occurs. For a radial deflection this motion produces  $N_s$  *satellites*, revolving around the accelerated equilibrium orbit (AEO) (Fig. 7). The *satellite* centers trace  $N_s$  evenly spaced cycloids in radial phase space hence  $N_s$  beam density modulation cycles for every one in the static case. A single *satellite* can be extracted by positioning a foil or septum deflector in one of the beam density minima. The separation between precession cycles decreases as  $N_s$  increases and as we move further from the resonance. Also phase dependent effects tend to wash out the coherence in the beam and so extracting closer to the resonance will give a cleaner time train<sup>o</sup>. The precessional component of the radius gain is reduced as  $N_s$  increases since a *satellite* is only radially separated from the other *satellites*, and hence extractable, near its maximum outward swing where the precessional component is minimum. Nonetheless the local beam density is reduced by at least a factor of  $N_s$  from the case where no perturbation is used.

A precessing coherent vertical oscillation produces a radial variation in vertical height of wavelength  $\Delta R = dR/dn/(\nu_z - \nu_z^*)$ .  $N_s$  such coherent *satellites* would produce  $N_s$  sinusoidal height variations uniformly spaced radially producing a height variation peak-

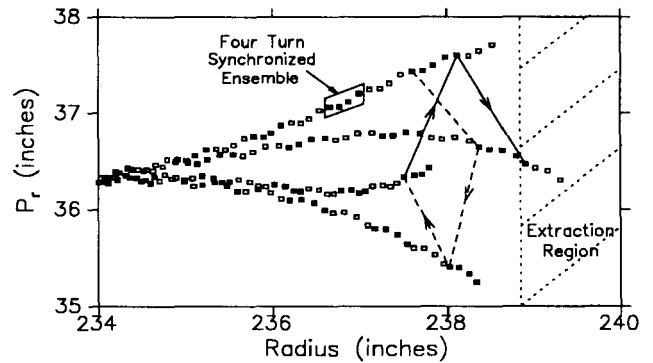


Figure 7: Single particle simulation result showing the growth and initial precession of particles at  $\nu_r=1.25$  ( $R \sim 237$  in.) in the TRIUMF cyclotron. Synchronized *mega-ensembles* composed of particles from four consecutive turns (highlighted by solid and empty boxes) trace out four separate *satellites* in radial phase space. The dashed and solid lines show the position of the particles on consecutive turns. An extraction region defined by a foil or septum extracts the leading *mega-ensemble*.

ing every  $1/N_s \cdot (\nu_z - \nu_z^*)$  turns. However single *satellite* extraction in the vertical space is more problematic and certainly, for septum extraction, less efficient due to the absence of any dispersion. Also  $\nu_z$  typically varies more with radius than does  $\nu_r$  resulting in a narrower resonance region and variations in the midplane in the extraction region are also problematic. Still, close to the resonance, before the precession in vertical space occurs, a foil or vertically deflecting septum placed just above the circulating beam could capture particles from a single *spoke*.

#### 4.3 Emittances of Resonantly Excited Beams

The stacking of micro-pulses in the time domain results in a corresponding increase in the energy spread and beam size, independent of incoming beam quality. Each rotating *satellite* comprises a *mega-ensemble* of particles from  $N_s$  consecutive turns with corresponding energy spread  $\Delta E_s \simeq (N_s - 1) \cdot E_g + \Delta E$  and radial width  $W_s \simeq \Delta E_s \cdot dR/dE + 2A_i$ , where  $A_i$  is the incoherent betatron amplitude and  $\Delta E$  is the energy spread in a single turn. An extracted four turn *mega-ensemble* created at  $\nu_r = 1.25$  is shown in Fig. 7. The precessional component reduces locally the normal  $dE/dR$  relation. The energy gain between extractions is  $E_G^* = N_s \cdot E_G$ . For mono-energetic incoming beams separated turns extraction may be possible, and extracted beams of energy spread  $\Delta E_s$  and radial width  $W_s$  result. For a uniform incoming beam the width of the extracted beam is  $W_{out} \sim E_G^* \cdot dR/dE$  and the extracted energy spread is  $\Delta E_{out} \simeq (E_G^* + 2A_i) \cdot dE/dR$ . In both cases the horizontal emittance is increased somewhat by precession. The

vertical emittance largely remains unchanged.

For vertical time-varying perturbations, extraction takes place over multiple turns. Therefore the energy spread and the radial width of the extracted beam are also dependent on  $N_s$ , but may be larger than in the radial case since more turns may be needed to capture all the beam. The vertical emittance is dependent on the  $N_s \cdot dz/dn$  coherent component driven by the deflecting field.

It should be noted that since the time-varying fields are periodic every  $N$  turns, emittance increasing resonance conditions may be driven by the gradient fields from the deflector. These should be analyzed by looking for resonance crossings on the tune diagram corresponding to the *super-orbit* of circumference  $2\pi N_s$ .

## 5 Resonant Extraction at TRIUMF

### 5.1 RF Deflector

At TRIUMF an rf device which excites coherent growth at  $\nu_r=3/2$  has been installed in the cyclotron since 1985. The RF Deflector (RFD) is well documented<sup>9,10,11</sup> and produces a sinusoidal radial deflection at 11.5 MHz ( $N_s=2$ ). A foil or septum placed in a beam density min-

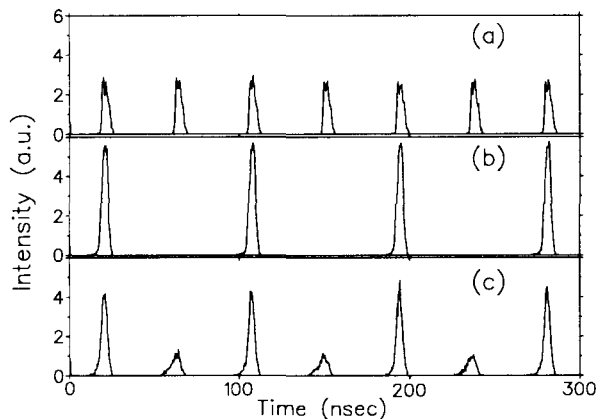


Figure 8: Experimental result showing the extracted time structure with and without the RFD ( $N_s=2$ ). In (a) with RFD off the bunches are separated by the normal period of 43 nsec. In (b) with RFD on the bunches are twice as bright and now separated by 86 nsec. In (c) the extraction foil is moved to extract a portion of beam from the neighbouring *satellite*.

imum will select from only one of the two precessing *satellites* in radial phase space. Consequently the period of the extracted pulses is doubled from the normal 43 nsec (23 MHz) to one pulse every 86 nsec (11.5 MHz) (Fig. 8). Typically the extracted energy spread increases from 1 MeV to 1.3 MeV and the radial emittance increases from  $1\pi\mu\text{m}$  to  $2.5\pi\mu\text{m}$  due to the precessional rotation of the coherent ensemble.<sup>9</sup> Close to the resonance the beam density minima are very stable and sufficiently

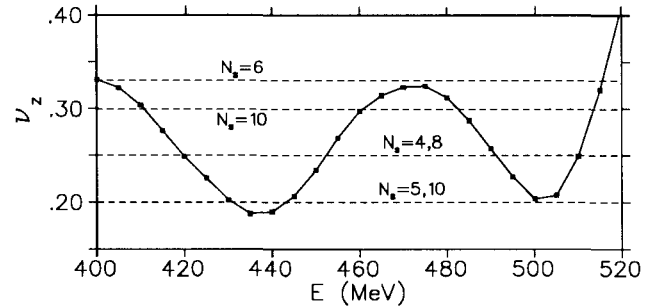


Figure 9: The vertical tune,  $\nu_z$ , as a function of energy for the TRIUMF cyclotron. The dotted lines correspond to  $\nu_z$  values where the noted  $N_s$  values would produce resonant conditions.

large so there is no problem maintaining this time structure. When the foil is placed near a transition between precession cycles the empty extraction bucket is again filled in proportion to the amount of beam sampled from the neighbouring *satellite* (Fig. 8(c)).

### 5.2 Pulsed Vertical Deflector

At TRIUMF a proposed  $\mu \rightarrow e$  conversion experiment<sup>12,13</sup> requires a pulsed beam with average intensity approaching 200  $\mu\text{A}$  at an energy of 500 MeV. Pulses of 100–200 nsec are desired with a period between pulses of 1–2  $\mu\text{sec}$ . This time structure can be achieved by using a pulsed deflector with pulses every five to ten turns (see Fig. 5). For extraction every five turns ( $N_s=5$ ) a value of  $\nu_r=1.2$  or  $\nu_z=0.2$  is required but at  $E=500$  MeV  $\nu_r > 1.5$ . The tune diagram in the outer radii of the TRIUMF cyclotron shows that there are many  $\nu_z$  values where resonant extraction is possible (Fig. 9). The horizontal dashed lines correspond to  $\nu_z$  values where the noted pulse period will yield a resonant condition (ie. where  $\nu_z \cdot N_s$  is an integer).

To optimize the efficiency of extracting a single coherent *satellite* vertically the extraction occurs at the resonance itself. The vertical deflecting plates are positioned so that the resonance coincides with the fringe field extending radially from the plates. With a vertical gap of 30 mm and the  $dR/dn$  of 1.5 mm, the beam will spend from 15–20 turns in the fringe field region (Fig. 10). The beam feels a periodic vertical perturbation of ever-increasing strength and the coherent amplitude grows over a narrow radial range in discrete jumps. A charge exchange extraction foil is positioned just above the circulating beam at an azimuth corresponding to a phase advance of  $\pi/2$  after the deflector. Whenever the acquired amplitude is sufficient to reach the foil the particle will be extracted and this will most generally correspond to a time directly after a pulse.

Computer simulation studies<sup>14</sup> were carried out to

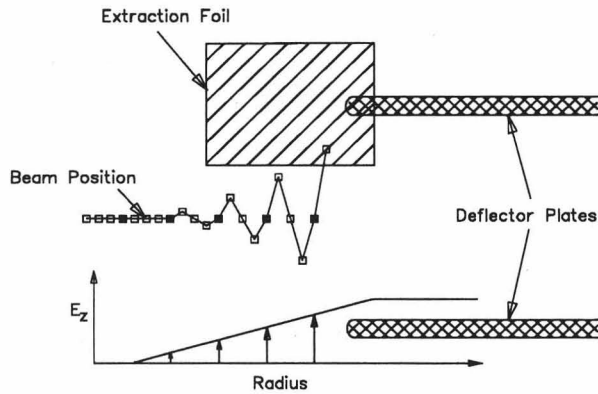


Figure 10: Schematic view of pulsed vertical extraction for the case where  $N_s=4$  and  $\nu_z=0.25$ . The small boxes correspond to the radial center and vertical height of the  $N_s$  turn wide *mega-ensemble* plotted once per turn. The darkened boxes correspond to times when the deflecting field is on. The profile of the fringe field is also shown with arrows indicating the average magnitude of the deflections. The ions are intercepted by the extraction foil after a phase advance of  $\pi/2$  in vertical phase space from the last deflection.

calculate the extraction efficiency, given as the percentage of the total beam extracted in synchronism to the driving pulse, the required deflector specifications, and the beam quality (including energy spread and transverse emittance) of the extracted beam. All studies were done using the Monte-Carlo, first order matrix tracking code, COMA.<sup>15</sup> Optimal deflector voltages (for a gap of 30 mm and 1 m length) and the corresponding extracted beam quality are shown in Table 1 for pulse periods ranging from  $N_s=4$  to  $N_s=8$ . The efficiencies are all  $\geq 99\%$  except at  $N_s=8$  where the efficiency is 97%. Particles extracted out of synchronism with the pulse could be removed in the extraction beamline by another pulsed deflector. As predicted the energy spread grows with pulse period. In addition a higher pulse period demands an increased deflector voltage for the same amplitude growth. The increased  $N_s \cdot dz/dn$  from a higher voltage yields a vertical emittance that increases with pulse period.

A FET based pulse generator has been designed<sup>16</sup>, fabricated and bench tested<sup>17</sup>. The specifications set for a pulse deflection test at  $N_s=5$  and  $\nu_z=0.2$  have been met.

Table 1: Optimized deflector voltages and corresponding extracted beam characteristics for various pulse periods,  $N_s$ .

$N_s$ (turns)	Voltage (kV)	$E$ (MeV)	$\nu_z$	$\Delta E$ (MeV)	$\epsilon_z$ ( $\pi\mu\text{m}$ )
4	6	492	0.25	2.9	1.3
5	9	499	0.20	2.7	2.2
6	15	478	0.32	3.8	2.2
7	18	486	0.28	3.7	3.1
8	18	490	0.25	4.3	3.4

Specifically a pulse magnitude of 10 kV at 0.92 MHz was achieved with flattop duration of 180 nsec. The rise and fall times of 40 nsec (Fig 11) correspond to the separation between TRIUMF bunches. A set of vertical deflection plates is presently being designed for a test with beam sometime in 1996.

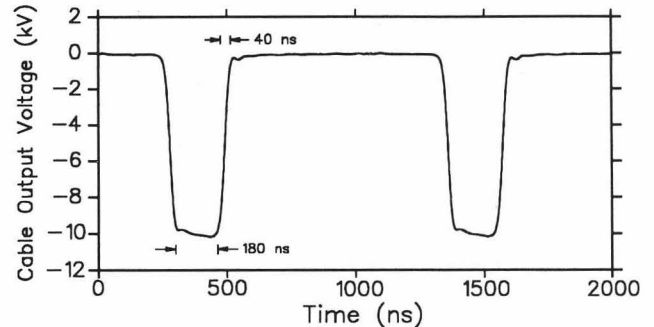


Figure 11: Measured output voltage from TRIUMF pulse generator.

## 6 Stacking Micro-pulses with a Pulsed Septum

A more straightforward way to generate a pulsed time structure is with a pulsed septum deflector.<sup>18</sup> When the field is off the beam is allowed to accelerate in the normal way into the deflecting gap.  $N_s$  turns can be accumulated before the pulse turns on for one orbit period to deflect all the accumulated beam onto a stripping foil or additional deflector positioned just outside the circulating beam (Fig. 12). The deflector gap must be large enough to accommodate the extra beam width. The efficiency could be improved by employing a precessional extraction technique. The beam quality of the extracted beams depends on  $N_s$  and on the details of the precession just as with resonant extraction.

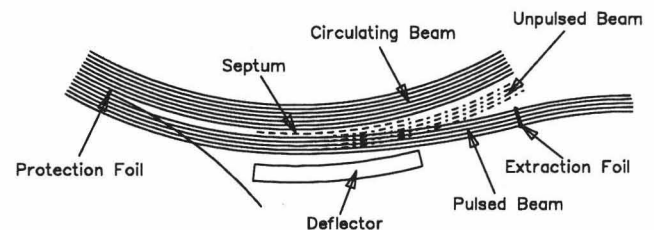


Figure 12: Schematic view of pulsed radial extraction. Here five turns are accumulated then all are deflected simultaneously onto an extraction foil. When accelerating  $\text{H}^-$  ions a narrow foil can be positioned upstream of the septum for protection.

The deflector voltage is determined from two factors: the field strength necessary to generate sufficient deflection and the deflecting gap required to accommodate the beam. Simulation studies<sup>18</sup> show that to stack

$N_s=6$  turns the final energy spread (2.8 MeV) and beam width in the deflector gap (15 mm) were increased over the unpulsed values (1 MeV and 5 mm respectively) by an amount given by the  $dE/dn$  of 0.32 MeV and  $dR/dn$  of 1.5 mm each scaled by the pulse period. The deflector voltage increases roughly linearly with pulse period to compensate both for the required larger gap and for the increased kick needed to clear the higher number of accumulated orbits.

The simulations show that at TRIUMF a pulsed voltage of at least 40 kV at 1 MHz is required to successfully stack  $N_s=6$  turns. This is beyond present technology<sup>19</sup>. The single, as opposed to multiple, deflection and the stronger radial focussing are the chief reasons for the higher voltage requirement when compared to the vertical resonant extraction scheme.

## 7 Modulating Bunch Population

It is also possible to use an additional rf cavity to modulate the population of the extracted bunches over a longer macro-cycle<sup>20</sup>. For example an accelerating cavity of harmonic  $m$  can be powered at a frequency  $\omega^* = m\omega_{rf} + \Delta\omega$  so the relative phase of the additional cavity with respect to the fundamental varies with frequency  $\Delta\omega$ . Depending then on the time of arrival at the cavity certain bunches will be accelerated and others will be decelerated, decreasing or increasing the over-all time of flight. The population of the extracted bunches will be modulated at the beat frequency. In an initial experiment using the fourth harmonic AAC cavity beat frequencies of 20–50 kHz were utilized. The intensity of the extracted beam was seen to vary at the beat frequency, with a peak to valley ratio of  $\sim 20$ , producing typical beam peaks of 4  $\mu$ sec FWHM separated by tens of  $\mu$ seconds. A chopper in the beamline could be used to produce a clean beam-off period in the time train.

## 8 Conclusions

In all such longitudinal manipulations Liouville's theorem demands the conservation of phase space. In these examples the chief result of redistributing particles in time is an increase in the energy spread of corresponding magnitude. In some cases the transverse emittance is also adversely affected. Charge exchange extraction certainly avoids any complications due to a loss of separated turns. It is then a matter of determining the acceptance limitation of the beam-line or post-accelerator to establish the allowed limits in the manipulation of longitudinal phase space.

## Acknowledgments

The author wishes to acknowledge the following people for their contributions to the content of this paper. G.H. Mackenzie originated the idea of the RFD as well as the concept and verification of the modulation of bunch population by rf beating. The concept of phase-splitting was developed in collaboration with W. Joho. The pulsed-deflection studies benefited from valuable discussions with W. Joho and R. Baartman. The author would also like to thank W. Rawnsley, L. Root and G.H. Mackenzie who helped with the beam experiments and G. Dutto for his support of this work.

## References

1. W. Yokota, *et al.*, Proc. 13<sup>th</sup> Int. Conf. on Cyc. and their Applic., Vancouver, 1992, p. 581.
2. R. Baartman, private communication
3. J.R. Delayen, *et al.*, Proceedings of the 1993 Part. Acc. Conf., p 1715, Washington, 1993.
4. R.E. Laxdal and W. Joho, Proc. European Part. Acc. Conf., p. 590, Berlin, 1992.
5. R.W. Mueller and R.W. Mahrt, Nucl. Instr. Meth, 86, 241 (1970).
6. W. Joho, Particle Accelerators, 1974, Vol. 6, p.41.
7. M. Zach, *et al.*, Proc. European Part. Acc. Conf., p. 973, Nice, 1990.
8. R.E. Laxdal, *et al.*, Proc. 13<sup>th</sup> Int. Conf. on Cyc. and their Applic., Vancouver 1992, p. 442.
9. R.E. Laxdal, *et al.*, Proc. 13<sup>th</sup> Int. Conf. on Cyc. and their Applic., Vancouver 1992, p. 415.
10. G.H. Mackenzie, Proc. 11<sup>th</sup> Int. Conf. on Cyc. and their Applic., Tokyo 1987, p. 222.
11. R.E. Laxdal, *et al.*, Proc. 11<sup>th</sup> Int. Conf. on Cyc. and their Applic., Tokyo 1987, p. 248.
12. S. Ahmad, *et al.*, Phys. Rev. D38 (1988) 2102.
13. C. Dohmen, *et al.*, Phys. Lett. B317 (1994) 631.
14. R.E. Laxdal, TRIUMF Design Note TRI-DN-94-35, Dec. 1994.
15. C. Kost and G.H. Mackenzie, Proc. of the Part. Acc. Conf., IEEE NS-22, p. 1922, 1975.
16. M. Barnes and G. Wait, Proc. of the 10<sup>th</sup> IEEE Intl. Pulsed Power Conf., Albuquerque, July 1995, to be published.
17. G. Wait and M. Barnes, Proc. of the 10<sup>th</sup> IEEE Intl. Pulsed Power Conf., Albuquerque, July 1995, to be published.
18. R.E. Laxdal, TRIUMF Design Note TRI-DN-94-27, Oct. 1994.
19. G. Wait, private communication.
20. G.H. Mackenzie, *et al.*, *A Demonstration of Beam Intensity Modulation without Loss of Charge*, these proceedings.